

## Examining the Subtropical Mode Water in the Southwestern Atlantic From in Situ Observations

M. B. Ferreira , O. T. Sato , P. S. Polito , and P. S. Bernardo 

Oceanographic Institute of the University of São Paulo, São Paulo, Brazil

### Key Points:

- Newly formed mode waters are distinguished by extremely low values of PV
- The formation of mode water is in phase with the time integral of the surface heat flux
- Mode water formation was triggered by a synoptic scale event (approximately equal to 5 days)

### Supporting Information:

- Supporting Information S1

### Correspondence to:

O. T. Sato,  
olga.sato@usp.br

### Citation:

Ferreira, M. B., Sato, O. T., Polito, P. S., & Bernardo, P. S. (2019). Examining the subtropical mode water in the southwestern Atlantic from in situ observations. *Journal Geophysical Research: Oceans*, 124, 2513–2526. <https://doi.org/10.1029/2018JC014762>

Received 14 NOV 2018

Accepted 22 MAR 2019

Accepted article online 29 MAR 2019

Published online 9 APR 2019

**Abstract** We investigated the formation and evolution of the South Atlantic subtropical mode water using data from profiling conductivity, temperature, and depth sensors (CTD) deployed in April–May 2015 and from two customized Argo floats that drifted from April 2015 to June 2017. From the CTD data, we observed a mode water layer below the seasonal thermocline that deepened from the southern side of the area to the north. The two Argo floats remained in the proximity of the cruise area for 2 years. Their slow displacement and recirculating patterns allowed us to observe the changes in the temperature and salinity structure before and after the formation period. We observed that the potential vorticity of newly formed mode water was  $O[10^{-1}$  to  $10^{-2}]$  of the mean value found in the whole mode water layer. There is a significant correspondence between the phases of the time integral of surface heat fluxes and the sea surface temperature. Mode water is observed to form at the integrated heat flux minimum phase. The relationship between the air-sea fluxes and sea surface temperature promotes the necessary preconditioning for the mode water formation. Once this was established, the outcropping of the mode water, that was at about 100 m depth, coincided with the passage of an atmospheric cold frontal system. This event suggests that the mode water formation can be triggered by the passage of cold fronts.

### 1. Introduction

Subtropical mode waters are a distinct volume of water with a remarkably low stratification located in the upper layers of the ocean. They are mainly formed from winter to midspring, a period characterized by severe weather conditions over the subtropical oceans with high intensity winds associated to low temperature and low relative humidity brought by the polar air masses (Marshall et al., 2009). The heat loss through the ocean surface results in a decrease of the water buoyancy. This promotes convective mixing in the upper ocean, deepens the mixed layer, and causes the outcropping of a previously formed mode water to the surface. Following that, the downward heat flux of late spring and summer stratifies the upper layer. The seasonal thermocline develops above that deep mixed layer, effectively isolating it from the surface, such that it accommodates between the seasonal and permanent thermoclines. Throughout the year, the submerged volume of mode water is subject to lateral advection and dissipation, resulting in its migration away from the formation region as the subtropical mode water decreases in volume (Douglass et al., 2013).

Globally, it is possible to identify the formation of mode waters in all oceanic basins (Hanawa & Talley, 2001). Among all the formation regions, the most widely explored are the North Pacific Subtropical Mode Water (Masuzawa, 1969), associated with the Kuroshio Current, and the North Atlantic Subtropical Mode Water (Worthington, 1972), called the Eighteen Degree Water (EDW) and it is associated with the Gulf Stream (GS). The oceanic heat loss to the atmosphere is responsible for the EDW formation (Kelly & Dong, 2013; Maze et al., 2009; Worthington, 1972). However, heat loss is not the only factor. Davis et al. (2013) used data from two moorings to conclude that the circulation and mixing of water properties from the GS contributes to the formation of EDW. The advection was particularly important in the convergence of warmer and saltier water in the formation region which changed the characteristics of the EDW in its early stages. Silverthorne and Toole (2013) deployed quasi-Lagrangian profilers in the GS region to observe changes in the heat storage in the upper ocean. During the winter the variations of heat storage in the mixed layer were dominated by forcing associated with the passage of severe storms. The authors observed that the heat stored in the mixed layer in typical EDW formation region is primarily controlled by advective processes due to the interaction with the GS.

In the South Atlantic, the subtropical mode water has its own peculiarities. The encounter of two western boundary currents and the thermodynamical forcing produced by the air-sea interaction processes favor its formation. The Brazil-Malvinas Confluence (BMC) occurs approximately between the latitudes of 36 and 38°S, where the warmer and more saline Brazil Current (BC) meets waters of the Malvinas Current of subpolar origin (Garzoli & Garraffo, 1989). East of BMC region, the southern edge of the subtropical gyre displays a steep northward deepening of the isopycnals toward the center of the gyre. Just north of BMC, the region next the main flow of the BC and its recirculation cell presents propitious conditions for the presence of mode water. This region is marked by a large net surface heat loss, it is still within the subtropical gyre and relatively protected from turbulent current fluctuations (Provost et al., 1999; Sato & Polito, 2014).

In contrast with the Northern Hemisphere basins, there are few studies that addressed the presence and evolution of the subtropical mode water in the South Atlantic. Gordon (1981) was probably the first to show in situ measurements of temperature and salinity profiles that depicted some mode water in the region. Later, Provost et al. (1999) searched for subtropical mode water using CTD and expendable bathythermograph (XBT) sections collected in the region from 1980 to 1996. This was the first time that the subtropical mode waters in the South Atlantic were analyzed and classified according to the same criteria used in the studies of mode waters from the North Atlantic and North Pacific. They found three types of subtropical mode waters in the South Atlantic basin. Adopting their nomenclature: STMW 1, the lightest kind located in a narrow zonal band around 33°S; STMW 2, in the BC Recirculation gyre; and STMW 3, the denser kind which is in the eastern side of the STMW 2. They did not identify mode water on the eastern side of the basin. More recently, Sato and Polito (2014) investigated the presence of subtropical mode waters in the South Atlantic based on the collection of temperature (T) and salinity (S) profiles obtained by Argo floats that sampled the region from 2002 to 2013. For that study, a much larger number of profiles, over 3,300, were included in the analysis of the mode water compared to the study performed by Provost et al. (1999). According to the cluster analysis presented in Sato and Polito (2014), the South Atlantic ocean exhibits three types of subtropical mode waters (SASTMW): one at the western boundary of the gyre near the BMC, a lighter one at the eastern side originated from the Agulhas current retroflexion, and a denser type at the subtropical frontal zone at the southern edge of the gyre. These mode water types are slightly different compared to Provost et al. (1999). Possibly, STMW 2 (Provost et al., 1999) is similar to SASTMW 1 (Sato & Polito, 2014). Also, some part of SASTMW 1 and SASTMW 3 was classified as STMW 3. In this study, we will follow the classification provided by Sato and Polito (2014) because of their more robust statistical analysis and the inclusion of a much larger data set.

The present work focuses on the results from the analysis of CTD and Argo data from one oceanographic cruise specifically planned to sample the subtropical mode water in the western side of the South Atlantic. In the next section we describe the data from the cruise and from two Argo floats that drifted in the region for 2 years. Sea surface temperature (SST) and height from satellites, and 10 m winds from model reanalysis, gave us a broader understanding of the physical processes that influence mode water formation and motion. Detailed analysis of these data gives us a better view of the outcropping and restratification cycle in the region of study. We examine the surface net heat balance in the region of study to establish the conditions where the mode water outcropped and subducted.

## 2. Data

Two in situ data sets were obtained thanks to an oceanographic cruise that took place between the 1st of April and the 8th of May 2015, carried out by the *Navio Hidroceanográfico(NHo) Cruzeiro do Sul* from the Brazilian Navy (Ferreira, 2019). That cruise was the first oceanographic campaign planned and conducted exclusively for the study of subtropical mode water in the South Atlantic. The deployment plan of the CTD stations was based on the evaluation of the most probable sites of the presence of the mode water. That determination was done using data from the In Situ Analysis System (Gaillard et al., 2009) developed by the “Laboratoire de Physique des Océans” from the “Institut Français de Recherche pour l'Exploitation de la Mer.” That data set is a tridimensional representation of the temperature and salinity of the global oceans obtained by means of monthly averaged data collected by CTDs, XBTs, and Argo floats by optimally interpolating them to a regular grid, between 2002 and present. The criteria developed for Sato and Polito (2014) for the detection of the subtropical mode water were applied to the In Situ Analysis System fields for the western side of the South Atlantic. Maps of the occurrences of the mode water were assembled for each month for the whole time series and the number of times that each grid point showed the presence of mode water was computed.

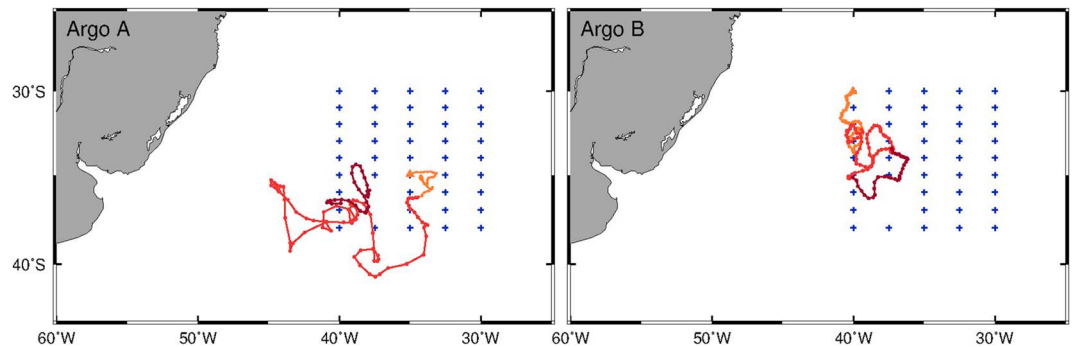


**Figure 1.** Area of study of SASTMW in the Brazil-Malvinas confluence region. Blue crosses show the location of the CTD casts from the April–May 2015 cruise. Circles (every 5 days) indicate the trajectory of profilers A and B between April 2015 and June 2017. The orange lines refer to the portion of the trajectory covered in 2015, light red in 2016, and dark red in 2017. The triangle indicates the deployment site of the profilers.

An index of occurrences of mode water at each grid was estimated by dividing that number by the total number of observations. Regions where this index exceeded 80% determined where the CTD stations would preferentially be deployed.

A total of 45 CTD casts were performed and ocean samples for further chemical analysis were collected simultaneously (Figure 1). Each CTD cast sampled the water column every  $\approx 3$  cm, from the surface to the depth of 1,000 m. The initial quality control of the TS profiles included the removal of spurious data that fall out more than three standard deviations from the mean values from adjacent profiles. The profiles were interpolated by bin-averaging in regular intervals of 1 m in the vertical to remove small scale features.

Two Argo profilers were deployed (Argo, 2018). Argo A (ID 5903130) was launched in the 26th of April at (35°W, 35°S) and Argo B (ID 5903131) in the 8th of May at (40°W, 30°S; Figure 1). These Argo floats had a parking level of 1,000 m and were programmed to emerge every 5 days as opposed to the conventional setting of 10 days. We consider that during the mode water formation, the ocean's buoyancy loss after the cooling by the atmosphere could promote a rapid convective mixing. Therefore, a shorter sampling cycle was set aiming for a better temporal resolution of the mode water during that period. To obtain a more detailed description of the upper ocean changes, the layer above 500 m had its vertical sampling set to 5 m. The formation of SASTMW only takes place from winter to midspring and only at some specific regions. The initial data provided by the salinity sensors on Argo A proved faulty and were discarded from the analysis (Figure 6, second panel). Salinities from the CTD and from the Argo profilers were converted and expressed as absolute salinity ( $S_A$ ) and temperature as conservative temperature ( $T$ ) (McDougall & Barker, 2011).

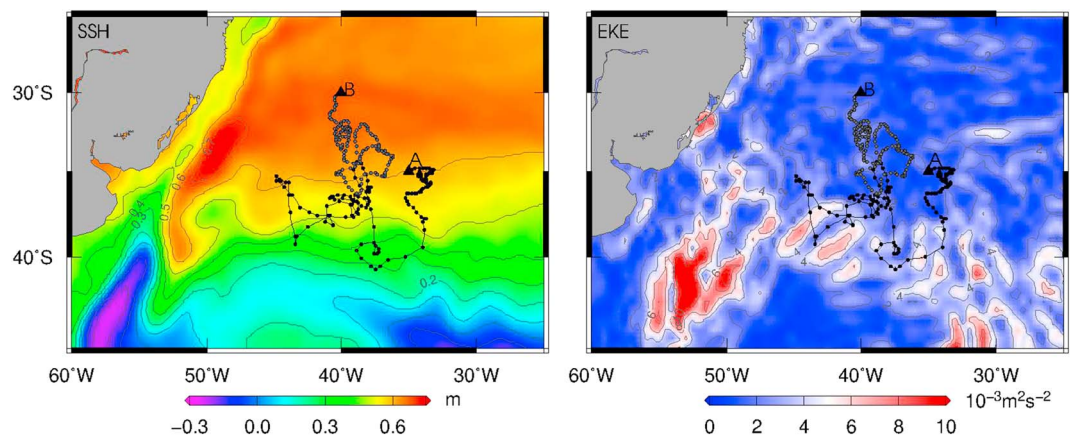


**Figure 2.** SSH (m) (left) and EKE ( $10^{-3} \text{ m}^2/\text{s}^2$ ) at the upper layer, estimated from altimeter data between 1993 and 2015, from Copernicus Marine Environment Monitoring Service, with the Argo trajectories superimposed. Triangles indicate the deployment sites. SSH = mean dynamic height; EKE = mean eddy kinetic energy.

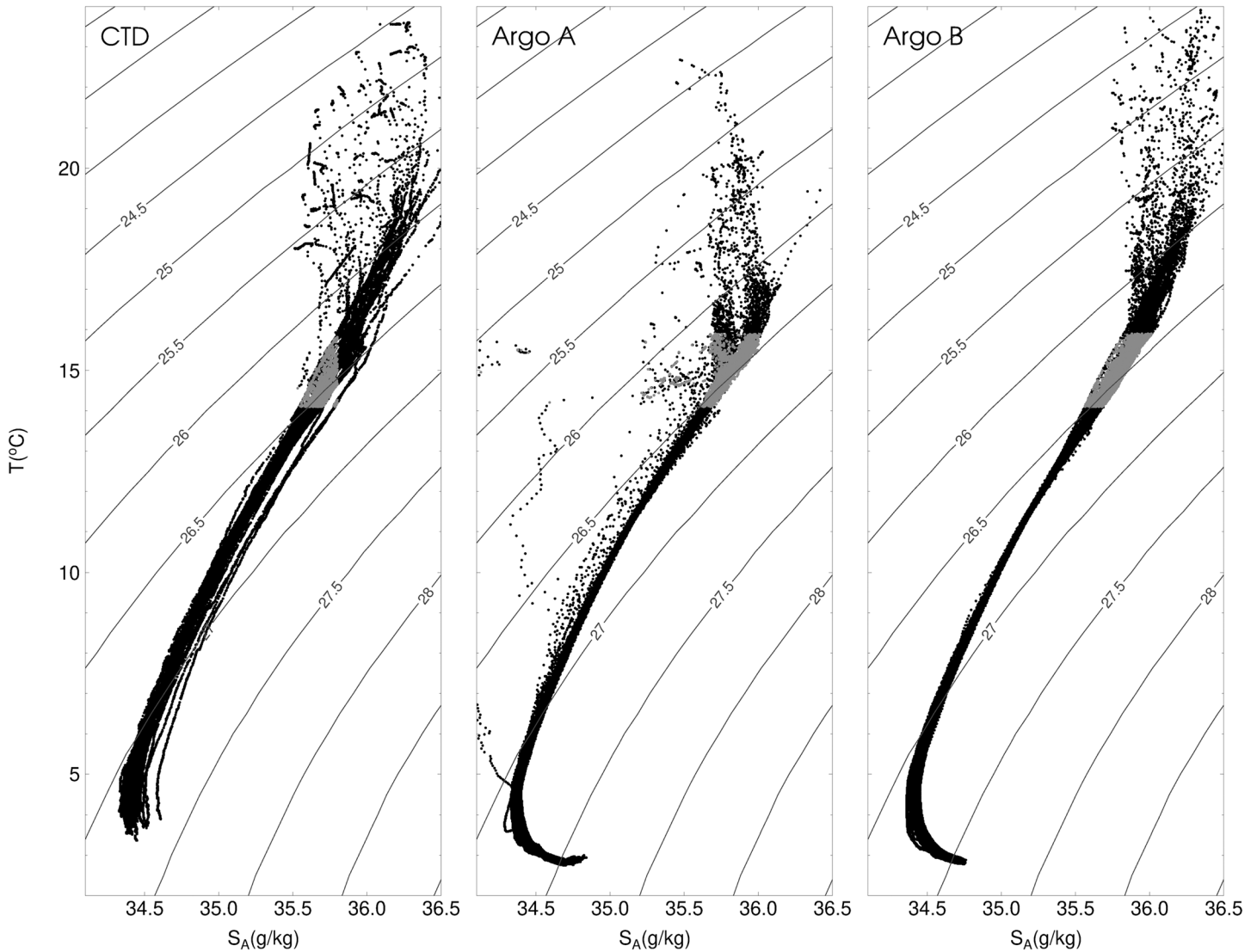


**Figure 3.** TS (conservative temperature/absolute salinity) diagrams for the CTD casts and for profilers A and B. The highlighted points represent the TS pairs that satisfied the identification criteria for the SASTMW. Thin contours of potential density  $\sigma_\theta$  are shown for reference.

Both Argo floats drifted within the area of study, displaced only a few hundred kilometers from their deployment sites 2 years after their deployments. The mean dynamic height (SSH) and mean eddy kinetic energy (EKE) maps, Figure 2, show a region of a relatively small sea level gradient associated with the small eddy variability. That would explain why the floats did not leave the region and, most importantly, why a mode water situation would be preserved over time.

We investigated the role of the surface heat fluxes during the formation of mode water. The data to estimate  $Q_{net}$  were obtained from the joint work from National Centers for Environmental Prediction (NCEP) and the National Center for Atmospheric Research (NCAR): the NCEP/NCAR Reanalysis Surface Flux data, (Kalnay et al., 1996).  $Q_{net}$  is estimated as  $Q_{net} = Q_{SW} + Q_{LW} + Q_{LH} + Q_{SH}$ , where the first two components are the shortwave and longwave radiative fluxes while the last two terms refer to the turbulent latent and sensible heat fluxes. All components are provided as global  $1.8750^\circ$  of longitude and  $1.9047^\circ$  of latitude maps of daily resolution. The time series span the period between 1948 and the present, of which we used data from 2015 to 2017. For reference, the sign of the heat flux is positive when the ocean gains heat from the atmosphere, that is, downward.

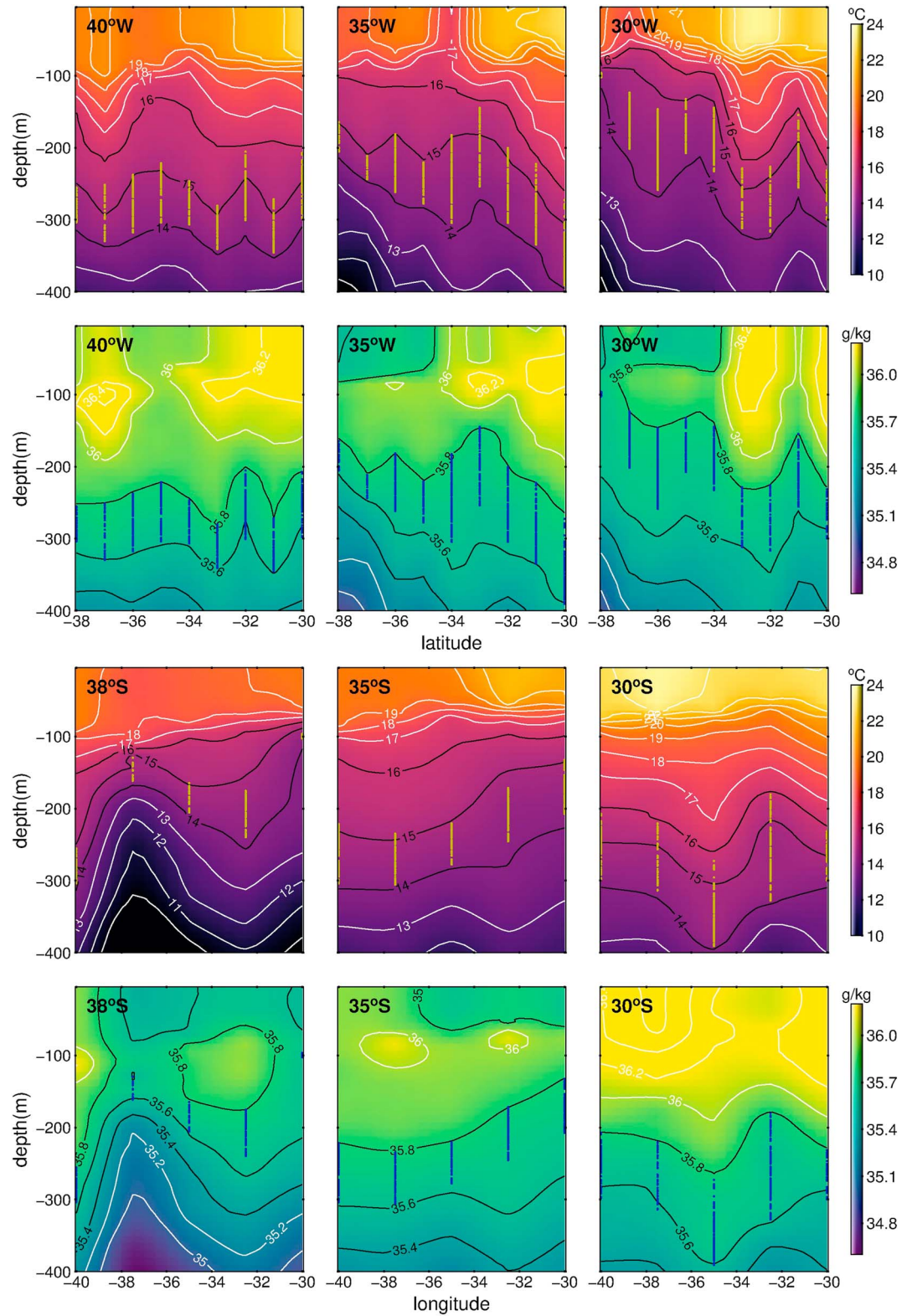


**Figure 4.** Temperature and salinity meridional sections at 40, 35, and 30°W (two superior rows), and zonal sections at 38, 35, and 30°S from CTD data. Small dots (blue and yellow) indicate the position in the profile where the mode water was detected. Black isolines indicate the contours used as detection criteria.

### 2.1. Identification Criteria

We applied the criteria established by Sato and Polito (2014) to the cruise data to identify the SASTMW type 1, the mode water on the western side of the basin near the confluence region. The temperature (T) range for the search is  $(15.0 \pm 0.9)^\circ\text{C}$ , and salinity (S) range is  $(35.6 \pm 0.2)$ . In addition to the thermodynamical criteria, we used the dynamical criteria of small potential vorticity (PV) required by the layer of low stratification in a region of negligible advection, defined by  $PV = \frac{f}{\rho} \frac{\partial \rho}{\partial z}$ , where  $f$  is the Coriolis parameter and  $\rho$  is the density of seawater. This is known as the isopycnic  $PV$  (Hanawa & Talley, 2001), a definition that retains only the vertical stretching component of the full PV. This component is affected by vertical exchange of heat and mixing that leads to mode water formation and destruction. Mode waters are required to have  $PV \leq 1.5 \times 10^{-10} \text{ m}^{-1} \text{ s}^{-1}$  along a continuous layer at least 100 m thick in the water column. After the initial quality control, the TS diagram of the CTD and Argo stations show the presence of mode water within the total TS range, gray dots in Figure 3.

## 3. SASTMW Observations From Cruise Data

The main objective of this study is to observe the SASTMW from in situ measurements. To accomplish that, hydrographic transects with CTD casts were performed between April and May 2015, as shown in Figure 1. In that time of the year we did not expect to observe the formation process that usually occurs between July and October, austral winter and midspring months. Therefore, the strategy for the cruise was to sample the upper layer of the ocean to establish if the mode water formed in previous years was present at subsurface and how deep and how thick it was. The detection criteria for the mode water were applied and identified a thick layer of homogeneous water with an average  $\sigma_\theta = 26.4 \text{ kg/m}^3$ , in agreement with Sato and Polito (2014).

Zonal and meridional transects across the sampled region show the deepening of the mode water layer toward the north. Figure 4 shows three meridionally oriented T and S sections (two top rows) from which the presence of the SASTMW between 100 and 400 m is evident and becomes thicker around  $34^\circ\text{S}$ . In the temperature sections, a well-defined mixed layer was observed in all sections, often between 0 and 80 m. Just below the mixed layer, a stratified layer corresponding to the seasonal thermocline tops the subtropical mode water layer.

In Figure 4 the presence of a well-defined mixed layer is more evident in the top 80–100 m in the temperature field in comparison with the salinity field. From the meridional sections, we questioned if the signal near ( $30^\circ\text{W}$ ,  $31^\circ\text{S}$ ) could be due to the presence of a mesoscale eddy. Sea surface height anomaly (SSHA) maps obtained from a combination of altimeters processed and distributed by the Copernicus Marine Environment Monitoring Service (CMEMS) were analyzed for the period of the cruise (CMEMS, 2018). Transient features of irregular shape in the SSHA were observed collocated with that signal. More striking is the feature at ( $38^\circ\text{W}$ ,  $38^\circ\text{S}$ ), where the T and S contours are vertically displaced at thermocline level, compressing the mode water layer. That is clearly associated with a nearly circular mesoscale eddy observed in the altimeter record (shown as supporting information). These two examples reinforce the idea that the SSHA are indicative of processes that change the thickness of the mode water.

Each T and S profile was analyzed for the presence of mode water. Once found, the depth of the upper and lower limits of the mode water are determined. Figure 5 shows the spatial distribution of these limits. The layer thickness of the mode water is obtained by the difference between the lower and upper limit depths. Our findings indicate that, during the cruise, the study area was characterized by the presence of submerged mode water. The mean layer thickness estimates considering only the mode water found in the CTD profiles is  $(80 \pm 32) \text{ m}$ . Observation of the position of the upper and lower limits of the mode water indicates that it is shallower in the southeast corner of the region and it deepens to the northwest (Figures 5a and 5b). The right panel on Figure 5 shows the total thickness of the mode water found from the CTD stations. We observed that near the center of the study region the layer thickness reached over 120 m. This thicker region can also be observed in the sections of Figure 4, in particular the plate for  $35^\circ\text{W}$ .

## 4. SASTMW Observations From Argo

Two custom programmed Argo floats were deployed during the cruise at sites where we expected to observe different stages of the mode water evolution, including its formation. These profilers drifted very little from

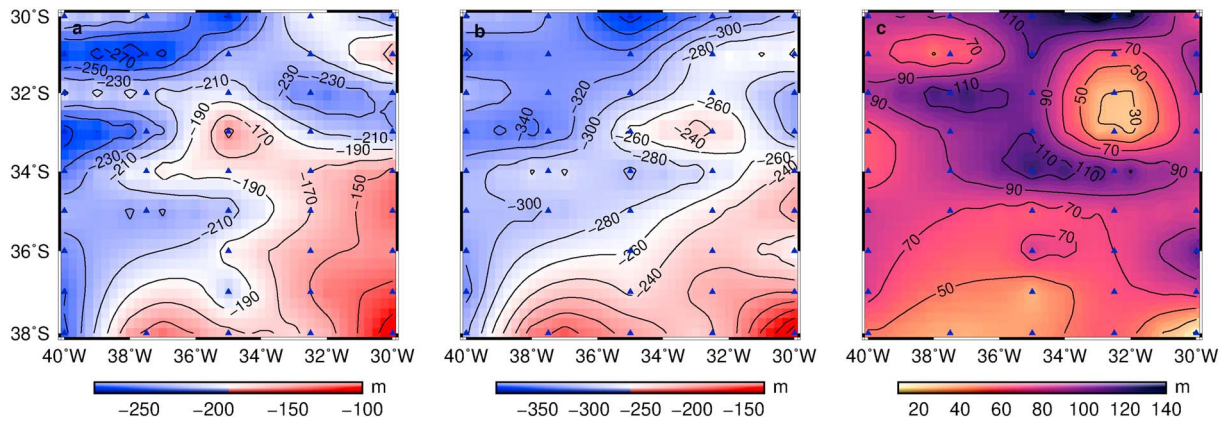


**Figure 5.** Depth of the upper (a) and the lower (b) limits of the mode water identified in the CTD data, and its layer thickness (c), in m. The triangles indicate the position of the CTD casts.

their deployment sites, about 300 km in 1 year (Figure 1). In both cases, their short displacement was associated with the fact that the region is characterized by weak mesoscale turbulence and weak mean flow advection, key ingredients to maintain a low PV layer. By moving so slowly, the data provided by the Argo floats made possible for us to observe the change in the ocean vertical structure or stratification, within the region where the SASTMW is found.

Argo A was launched approximately at the center of the study region. At the deployment time, the upper ocean structure had a warm and homogeneous mixed layer that occupied the top 70 m approximately (Figure 6 add yellow line at top panel). From the depth-time diagrams, the isotherms in the range of the mode water,  $(15.0 \pm 0.9)^\circ\text{C}$ , were detected between 100 and 300 m from April to late July 2015. Following the T and S time series of Argo A (Figure 6, top 2 panels), the cooling (and to a lesser extent, freshening) of the mixed layer between August and early November 2015 becomes quite evident. Even though the observations provided by the Argo are not at a fixed location, its relatively short displacement can be considered stationary enough for this particular analysis. By the end of August 2015, the  $16^\circ\text{C}$  isotherm outcrops at the surface, exposing the preexisting mode water to the atmosphere. Only by November the surface layer starts to restratify and isolates a thicker layer of mode water to the subsurface if compared, for instance, to its thickness in July. After November, the first and third diagrams on Figure 6 clearly show the development of the seasonal thermocline above that homogeneous layer. The signature of the seasonal thermocline can be clearly seen as high values in the PV diagram (dark red,  $PV > 8 \times 10^{-10} \text{ m}^{-1} \text{ s}^{-1}$ ). The layer above 300 m presents salinity between 35.4 and 35.6. Changes in the salinity structure became more evident after float A moved toward the south of  $38^\circ\text{S}$  in April 2016, moving through the subtropical front.

The third panel of Figure 6 shows the PV evolution along the Argo A trajectory. The points in the Argo profiles that satisfied the condition presented in section 2.1 are marked in this diagram. The gray circles represent the data points where all SASTMW identification criteria were satisfied. The location of the mode water is corroborated by the data provided by the CTD casts, Figure 4, at  $(35^\circ\text{W}, 35^\circ\text{S})$ .

Earlier in the time series, when the shallow mixed layer was present, the mode water was found just below the layer of higher PV, which was in the range of  $(4 \text{ to } 6) \times 10^{-10} \text{ m}^{-1} \text{ s}^{-1}$ . From the temperature panel we find that these PV values correspond to the stratified layer associated with the remains of a weak seasonal thermocline. The outcropping of the submerged isotherm marks the opening of the ventilation window where the lower layers of the ocean become exposed to the atmosphere.

In Figure 6, third row, we identify formation from late August to early November 2015 and July to October 2016. In that, the so-called mixed layer became thick, spanning from the surface down to 290 m. The deepening was the combination of new homogeneous water injected on top of the preexisting mode water. In 2015, between 150 and 200 m, we can observe a thin and intermittent discontinuity in the points between the newly formed mode water above the old one. Compressed between both layers, note that this thin layer has a slightly higher PV compared to the values of the mode water above or below it. During the course of the formation period, this layer is homogenized and incorporated within the total volume of mode water.

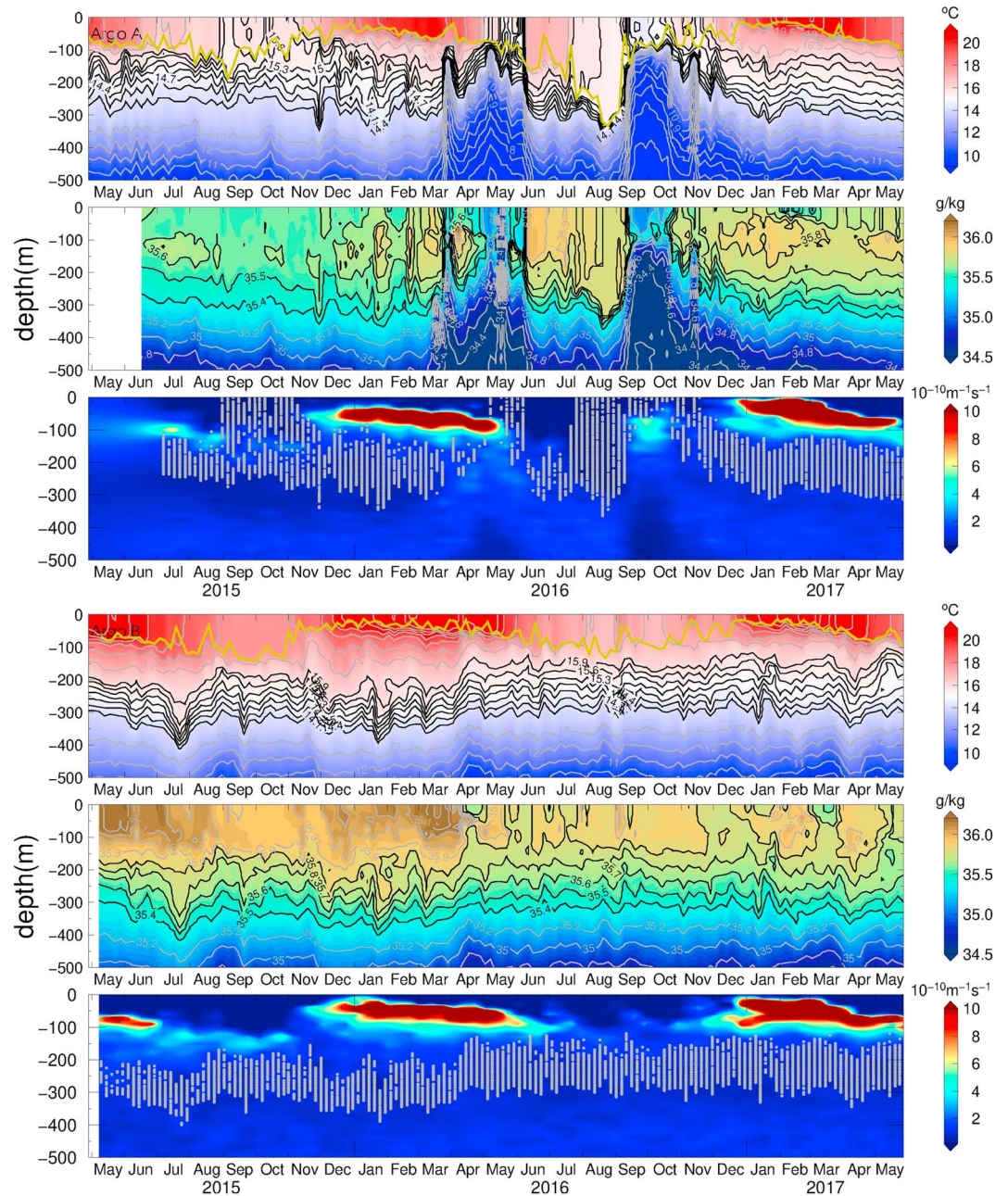


**Figure 6.** Depth-time diagrams for temperature (red-blue), salinity (blue-yellow), and potential vorticity (dark blue) for Argo A (ID 5903130; three upper panels) and Argo B (ID 5903131; lower). The gray circles and the contours represent the points in the profiles that satisfied the selection criteria for mode water. The yellow lines indicate the depth of mixed layer using de Boyer Montégut et al. (2004) criterion.

The mean temperature within the mode water layer sampled by Argo A is  $(15.1 \pm 0.5)^\circ\text{C}$ , shown in Figure 7a, and the mean salinity is  $(35.8 \pm 0.1)$ . A large portion of the T and S variability of the mode water came after the formation window when Argo A started to drift further south. During the formation period of late August to mid-November of 2015, the mode water layer thickness increased as it outcropped. The introduction of slightly warmer surface waters elevated the mean temperature of the whole mode water layer. During this period, the mean layer thickness was  $(243 \pm 29)$  m, but reached as deep as 280 m and the mean T of the mode water was  $(15.2 \pm 0.1)^\circ\text{C}$  while the mean S was  $(35.70 \pm 0.01)$ . Just 2 months earlier, the mode water layer was  $(101 \pm 26)$  m thick with a mean T of  $(14.6 \pm 0.1)^\circ\text{C}$ . During 2 months after the formation, the layer became  $(170 \pm 56)$  m thick and the mean T was  $(14.8 \pm 0.2)^\circ\text{C}$ . The mode water mean salinity remained

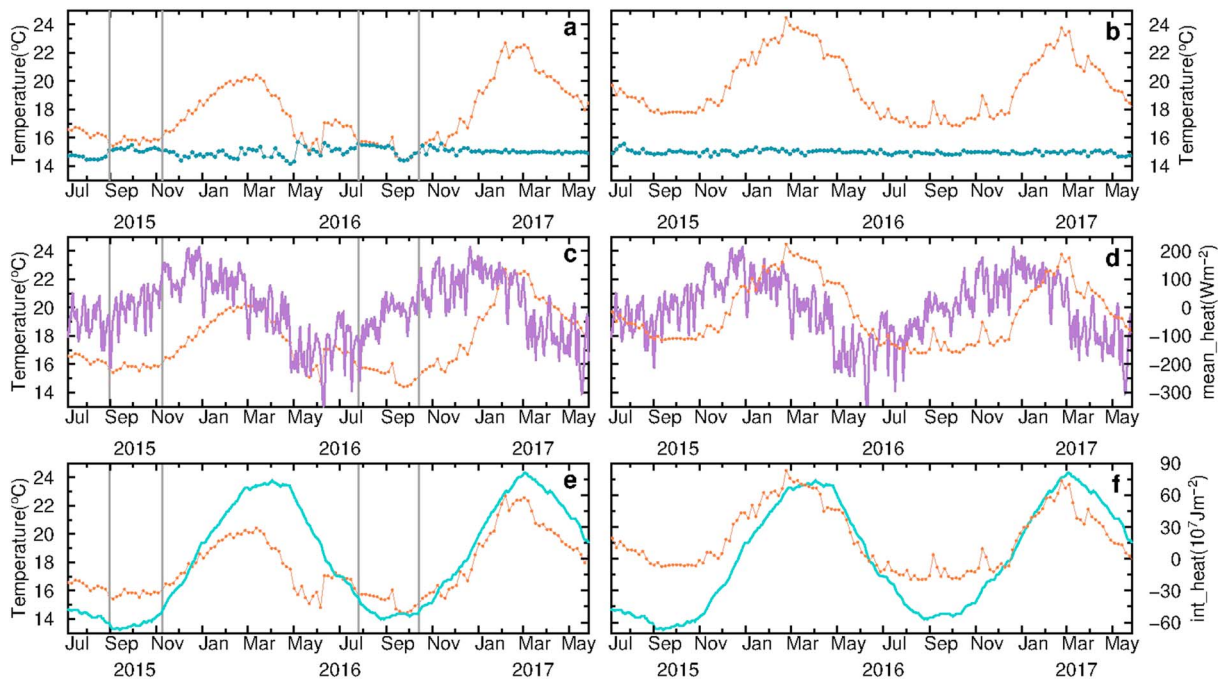


**Figure 7.** Sea surface temperature measured by Argo (orange lines). Left panels refer to Argo A, and right, Argo B. (a and b) Blue lines refer to the mean temperature ( $^{\circ}\text{C}$ ) within the SASTMW. (c and d) Purple lines represent the mean net surface heat flux balance ( $\text{W}/\text{m}^2$ ). (e and f) In cyan, the time integrated mean surface net heat flux ( $\text{J}/\text{m}^2$ ). The vertical gray lines in the left panels bracket the “formation periods.”

stable during that whole period. Furthermore, the waters injected into the preexistent SASTMW volume (i) have lower PV, and (ii) are slightly warmer. We take these as indications that a convective process took place and it homogenized waters from above. Therefore, we ruled out that the warming observed during formation period could be due to influence of some lateral advection (Davis et al., 2013). In addition, Figure 2 suggests that during this period, the profiler was in a relatively calm region, a scenario that reinforces the previous argument.

The newly formed mode water layer was in contact with the atmosphere and had a relatively smaller PV than the rest of the mode water. The average PV for that layer was  $2 \times 10^{-11} \text{m}^{-1} \text{s}^{-1}$ , but reached as low as  $2 \times 10^{-12} \text{m}^{-1} \text{s}^{-1}$ . Thus, this secondary criteria is useful to identify the mode water that just formed. The presence of reduced values of PV during the formation events corroborates Forget et al. (2011) assumptions when they used a numerical model to investigate the EDW. Here we provide a confirmation of the usefulness of such lower PV values using in situ data to identify newly formed waters.

After November 2015, the gradual diabatic heating of the surface waters promoted the restratification of the upper layer as indicated by the Argo A temperature record (Figure 6 top panel). The establishment of the seasonal thermocline is pronounced in the PV time series with large values ( $\text{PV} > 10 \times 10^{-10} \text{m}^{-1}/\text{s}$ ) in Figure 6, third panel, between 50 and 100 m. This seasonal thermocline is much stronger (thicker and more stratified) compared to the deeper and thinner seasonal thermocline observed just before the formation period. Above the new seasonal thermocline, a thin mixed layer becomes noticeable. Evidently we cannot make any assumptions about the volume of mode water formed from a single Argo float. However it is noteworthy that the layer thickness of the mode water after the formation event is larger compared to the period before, in that region. From the trajectory plotted in Figure 1, the float left the cruise region after mid-March 2016. The change in the dynamics regime can be assessed in the depth-time diagrams. In the PV diagram, very few points that attend the mode water criteria were found.

Between May and November 2016, Argo A trajectory (Figure 1, left) presented relatively quick displacements, as it reached a region characterized by faster currents and higher EKE. The consequence of these displacements is shown in Figure 6 as two periods with rather quick elevation of the coldest isotherms and freshest isohalines that mark two crossings of the subtropical front in Figure 2, left. In June 2016, Argo A reentered the cruise region from the southwest corner and drifted north-westward. Once again, it recorded

the beginning of a new formation cycle of mode water. In 2017 the float returned to the low-EKE region and a new cycle of cooling and deepening of the mixed layer is observed, yet records ceased before the 16 °C isotherm could outcrop.

Argo B was launched near the northwestern edge of the transects region. It drifted about 500 km to the South from its deployment site within 1 year, Figure 1 right panel. The temperature depth-time diagram in Figure 6, fourth panel, shows a warmer upper layer temperature compared to Argo A because it was further northwest, under the influence of the BC. However, the temperature calculated within the mode water layer (gray dots in bottom panel) was the same as Argo A's ( $15.0 \pm 0.1$ ) °C and the mean salinity was ( $35.60 \pm 0.04$ ). In April 2015, the isotherms within the mode water range can be identified between 205 and 300 m, deeper compared to the same period of Argo A, confirmed by the data collected by the CTD cast, Figure 4 sections at 40°W and 30°S. At that time, we observe a warmer mixed layer and also a thicker seasonal thermocline above the mode water. From April to August 2015, the temperature of the mixed layer decreased, and in mid-August the 18°C isotherm is exposed to the surface. This happens because during the winter a thick mixed layer develops progressively but the preexisting mode water was never exposed to the atmosphere. This is more evident in the PV diagram (Figure 6, bottom panel) as a band of high values above 100 m. The temperature of the mixed layer is higher (above 20 °C) compared to Argo A. After November, the warming of the surface temperature starts the process of restratification of the upper layers, forming again the seasonal thermocline (dark red,  $PV > 8 \times 10^{-10} \text{ m}^{-1} \text{ s}^{-1}$ ).

The Argo B salinity record starts earlier in comparison with Argo A and presents evidence of a salty and well-defined mixed layer from the beginning of the diagram until July 2015. From August to November 2015, there is a freshening of the upper layer, from the surface to about 160 m. Afterward, the restratification process mimics the temperature patterns. From mid-June to November 2015, the seasonal thermocline disappeared, replaced by a mixed layer that extends only to about 120 m, approximately limited by the depth of 17 °C isotherm. By spring, the cycle of restratification restarts, forming a discrete seasonal thermocline between 50 and 100 m (Figure 6, bottom panel). The salinity field was not as homogeneous compared to Argo A, even though during winter, within the mixed layer the salinity varied less than 0.05. From the point of view of Argo B, during the formation period the preexisting mode water was never exposed to the atmosphere; the ventilation window was not deep enough to reach its upper limit. The PV diagram displays the samples that satisfied the identification criteria and all of them were below the depth of 150 m. The mean thickness of this layer was ( $124 \pm 24$ ) m.

From winter up to midspring, July to November 2015, the low values of PV are observed in the mixed layer but the T and S values did not correspond to the expected values for the mode water, Figure 6, three lower panels. In the Argo B trajectory (Figure 1, right) a slow southward drift of approximately 4.3° is observed in 2016 and 2017. This corresponds to the upward displacement of the isopycnals in the fourth panel of Figure 6, accompanied by freshening of the layer above  $\approx 250$  m. The layer of submerged mode water (Figure 6, bottom) also moves upward, as expected. Despite that, no formation of SASTMW was observed. In fact, just below the low PV ( $< 1.0 \times 10^{-11} \text{ m}^{-1} \text{ s}^{-1}$ ) region there was a thin layer of slightly higher PV of about  $5.0 \times 10^{-10} \text{ m}^{-1} \text{ s}^{-1}$ , the remnants of the seasonal thermocline, separating the mixed layer from the mode water. The isolation of the mixed layer is confirmed by the observation that the thickness of the mode water layer remains constant, in contrast with the PV analysis of the Argo A data. Therefore, for Argo B, although the mode water was present throughout its trajectory, it was never exposed to the surface.

Overall, both Argo floats pictured distinct regions occupied by the mode water in the South Atlantic. Their slow displacement during the course of about 24 months and their contrasting results allowed us to analyze the changes in the vertical structure of the upper layer. Argo A captured the outcropping of the mode water isotherms and the restratification of the ocean after the closure of the ventilation window. Just before the formation, zooming in Figure 6 top panel, the convective mixing makes the isotherms plunge almost vertically from surface to the mode water while afterward, the restratification gradually reorganizes the isotherms during the warming months. The customized Argo had a temporal resolution of 5 days. Thus, it seems fair to conclude that the heat exchange between ocean and atmosphere in June and July, the 2 months that preceded the SASTMW formation, have homogenized and cooled the upper layer (above  $\approx 150$  m in 2015, above  $\approx 220$  m in 2016). This preconditions the upper layer, increasing its potential energy, such that another event that occurred within the atmospheric synoptic time scale, for example, a frontal system or a cyclone, has triggered the fast convective process in the ocean observed in the first days of September 2015. This is an

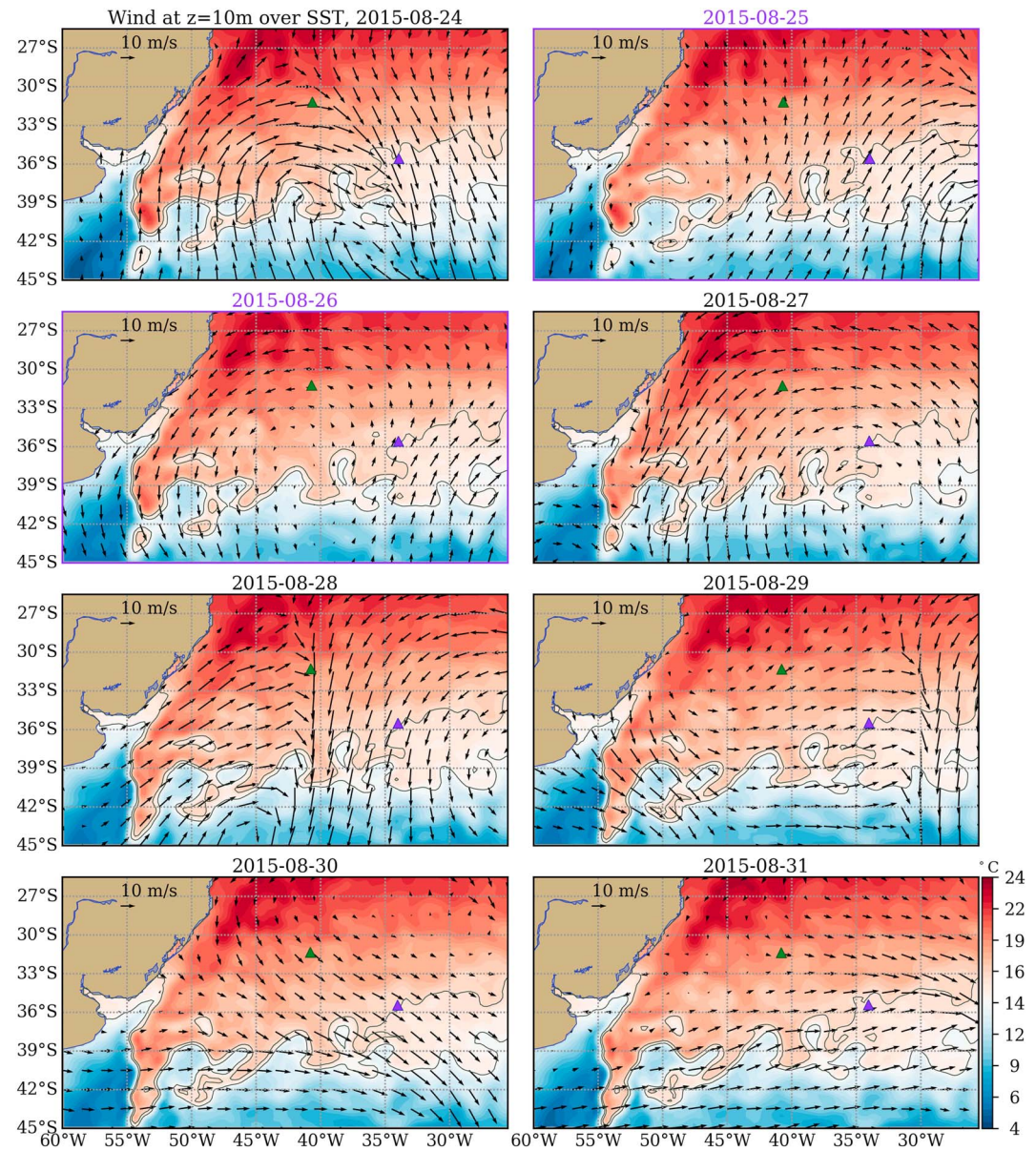


**Figure 8.** Daily (24–31 August 2015) mean sea surface temperature maps superposed by wind vectors. Contours indicate 14.1 and 15.9 °C isotherms, temperatures that bracket the SASTMW. Triangles show the position of Argo A (purple) and B (green).

additional evidence that heat exchange is more important for the SASTMW formation than advection in the region of study. Meanwhile, Argo B did not experience the formation of mode water, it rather stayed during the whole time in a region where the SASTMW was present at depth.

To examine the idea of formation driven by air-sea interaction, we analyzed the daily winds from the ECMWF Reanalysis Interim product (ERAi; Dee et al., 2011) and the daily SST from the Reynolds (OI-SST) data (Banzon & Reynolds, 2013). These are combined in Figure 8 that shows also the positions of Argo A and Argo B between the 24th and 31st of August 2015. The gray lines depict the contours of  $(15.0 \pm 0.9)$  °C that mark the SASTMW temperature range. Argo A is located at the edge of the marked region, while Argo B is about 600 km to the NW. The wind was blowing from the NW on the 24th, thus from warm to cold SST over Argo A. The wind turns and during the next 2 days (purple frames on Figure 8) it blows from SSW, thus from cold to warm SST. During the rest of the period it changes direction often but keeps going from warm to cold SST regions over Argo A. The wind is often above 10 m/s throughout the period, yet on the 24th and 25th

it brings cold air from the south and that supports the idea that this change in the atmospheric conditions triggered the mode water formation where Argo A was located. By the 31st Argo A emerges approximately in the same position, however it is south of the 15.9 °C contour because the isotherm moved northward. From the ocean's interior perspective, the isotherm's displacement can be interpreted as the outcropping observed in August, 31st, in the upper panel in Figure 6. Thus, it seems that the leading factor in this case was the air-sea heat flux and not the lateral advection.

## 5. Relationship Between Formation and the Heat Flux Cycle

We would like to address the differences observed by these two Argo floats and to understand what mechanisms contribute to the variability of the mode water. For that, we will examine the regional patterns of some dynamical and thermodynamical parameters. Would the formation of mode water, a process in which the ocean loses heat (Worthington, 1972), be in phase with its annual cycle? By following single drifters one could examine this relationship as a function of time. To address this question we analyzed the net heat flux balance ( $Q_{net}$ ) and its time integral ( $Q_{int}$ ) along the trajectory of the floats. We estimated a time series (2015–2017) of the mean surface net heat flux balance averaged within an area that encompasses the two profilers: 30 to 49°W, 26 to 45°S. That time series was compared to the SST and mode water mean temperature obtained by the profilers, as shown in Figure 7.

The upper panels on Figure 7 compare the variability of the SST relative to the mean temperature in the mode water layer. The latter does not depict significant changes in consonance with the seasonal cycle, although we observed that the layer thickness adjusts with the input of newly formed mode water, Figure 6. In the middle panels of Figure 7, the annual cycle of  $Q_{net}$ , averaged over the area mentioned above, shows high frequency variability at daily scale and an annual amplitude of  $(266.7 \pm 0.1) \text{ W/m}^2$ . It is conspicuous that the  $Q_{net}$  annual cycle is out of phase compared to the SST cycle for both instruments, Argo A and B. In addition to that, during most part of the formation period, from August to November 2105, and July to October 2016, the net heat flux was on average positive during the path of Argo A. This would be contradictory considering that we would expect heat loss during formation. However, in the preceding months  $Q_{net}$  was predominantly negative.

To evaluate the cumulative effect of net heat balance in the ocean, the daily mean NCEP net heat flux was integrated over three annual cycles, from 2015 to 2017, and detrended.  $Q_{int}$  time series is shown in the lower panels in Figure 7 compared to the SST time series. It shows as a smooth curve compared to  $Q_{net}$  because it accumulates the effect of the annual heating and cooling cycle. It became evident that even though the net heat flux was mostly positive during the formation period, in this case the spring season in the austral hemisphere, the integrated variable  $Q_{int}$  accounts for thermal inertia over time. This could explain why the annual cycle of SST and  $Q_{int}$  are in phase and the formation period coincides when both time series are near their minima. In this case,  $Q_{int}$  worked to precondition the oceanic heat reservoir to generate mode water. That occurs during the spring months when both the stratification and the SST are low enough to permit that synoptic atmospheric systems to trigger a deep convective mixing process that generates mode water, and drastically reduces PV over a period of a few days.

As stated before, Argo B was not in a region of formation; this lead us to conclude that the relatively small fluctuations on mode water properties it registered, Figure 6, were most likely due to lateral advection. The SST time series on the left side of Figure 7 was never as low as the mode water temperature, as seen in Argo A. That would be a necessary condition to form mode water since potentially both floats were under very similar conditions relative to  $Q_{net}$  and  $Q_{int}$ . An important preconditioning element missing for SASTMW formation was a colder SST that could enable the outcropping of submerged isotherms.

## 6. Conclusions

In this study we examined in situ data from by a hydrographic cruise that took place between April and May 2015 northeast of the Brazil-Malvinas confluence region. This cruise aimed two objectives: (i) Assess the oceanic conditions that characterize the presence of the subtropical mode water in the South Atlantic and (ii) launch two customized Argo floats that, if they remained long enough around the region, would allow us to increase our knowledge about the mode water development cycle.

A total of 45 CTD casts were made during the cruise. After the quality control, the mode water selection criteria were applied to each profile. The criteria of SASTMW identification is temperature in the range of  $(15.0 \pm 0.9)^\circ\text{C}$ , and salinity range of  $(35.6 \pm 0.2)$ , and  $PV \leq 1.5 \times 10^{-10} \text{ m}^{-1} \text{ s}^{-1}$ . From the analysis, the mean thickness was  $(80 \pm 32) \text{ m}$ . The upper limit of this layer was the shallowest in the southeastern corner of the cruise array and deepened to the northern side. The timing of the cruise was planned to observe the submerged SASTMW formed on the preceding years. The formation process takes place from winter to midspring (July to October in the austral hemisphere, ; Sato & Polito, 2014). Two Argo floats were deployed in the region to continue sampling the upper layers of the ocean. They were programmed to have a repeating cycle of 5 days and a higher resolution sampling of the first 500 m of the water column. By doing that, we allowed the instruments to capture in detail the rapid changes that occur during the winter's convective mixing.

The two Argo floats were launched during the cruise and they ended their missions after 2 years, within the vicinity of the BMC. Even though we were twisting an Eulerian view from a Lagrangian instrument, the time series provided by these slow moving floats helped us to observe the different paces at which the changes in the temperature and salinity structure of the upper ocean that precede and follow the formation of SASTMW occur. Argo A was launched near the center and Argo B at the northwestern corner of the cruise array. They captured very different aspects of the spatial and temporal distribution of the mode water.

For almost 1 year, while still within the domain of the cruise array, Argo A provided data to observe the rapid ( $O[5 \text{ days}]$ ) cooling of the mixed layer, the outcropping of the  $16^\circ\text{C}$  isotherm which exposed to the atmosphere a preexisting layer of mode water at depth, and the slow ( $O[30 \text{ days}]$ ) restratification of the upper layer by the beginning of the summer. The PV analysis is useful to map the presence of the mode water at the submerged stage but also at the beginning of the formation process. At the latter, the mode water layer thickness reaches its maximum during the year. The PV mapping also reveals that the most recent mode waters have much lower PV values, ( $PV < 2 \times 10^{-11} \text{ m}^{-1} \text{ s}^{-1}$ ), compared to the older ones. This empirical observation establishes that a very low PV can be used to distinguish newly formed mode water from the rest. Here we can introduce the idea of the "thin cushion" as a layer that has a slightly higher PV, and separates two bodies of SASTMW formed in consecutive years.

The analysis of heat fluxes along the floats' trajectory addressed some of the questions about the role of the energy exchanges between the oceanic upper layer and the overlying atmosphere. First of all, the formation period does not necessarily match the time when the surface heat balance is negative. Specifically for Argo A, when the formation took place it was already spring and the heat flux was mostly positive, that is, the ocean was, on average, gaining heat. However, in the preceding months the heat balance was negative. The phase of the time integral of the surface heat balance matches the timing of the formation period. That indicates that the formation in this region is driven by air-sea interactions with a lag relative to the immediate heat flux balance. At least in the particular case of Argo A, the interaction that triggered the formation of mode water in 2015 occurred on a synoptic (atmospheric) time scale.

Argo B was launched in the vicinity of the BC recirculation gyre, a warmer region compared to the center of the array. Argo B never left the region of the cruise and it never reached a region where it could sample the formation process. Its 25-month long time series shows a  $(124 \pm 24) \text{ m}$  thick layer of mode water at subsurface, between the seasonal and the permanent thermoclines. It traveled in a region that does not hold some primary conditions to support mode water formation that could be summarized as the upper layer being too warm. This implies that the potential energy of that layer is too low to permit a deep convective process to be triggered by a front or cyclone. In a more colorful language, it locks the trigger. Because of that, the submerged layer was not able to outcrop during that winter and neither in the following year. Even without a connection with the atmosphere, the layer thickness and depth of the mode water showed some relatively small temporal variability. This could lead us to speculate that these changes are correlated to adiabatic processes tied to the BC dynamics rather than air-sea interaction.

To sum up, in situ data were essential to the analysis of the SASTMW. The CTD array established the foundation of the mode water structure in the region. The observation of its life cycle was only possible because of continuous measurements promoted by Argo profilers. The custom profilers were decisive to distinguish two distinct dynamical regions in terms of mode water formation. Formation was only observed South of  $34^\circ\text{S}$  while the mode water was present at subsurface almost everywhere. The mode water is formed at

these windows that quickly open by the end of winters and spreads northward toward the center of the gyre afterward. These newly formed waters have a remarkably low PV signature.

### Acknowledgments

The authors wish to thank the Brazilian Navy for making the cruise and the deployment of the two Argo float possible. The profilers' data were collected and made freely available by the International Argo Program and the national programs that contribute to it (<http://www.argo.ucsd.edu>, <http://argo.jcommops.org>). The Argo Program is part of the Global Ocean Observing System. ISAS temperature and salinity products were produced and distributed by the French Service National d'Observation Argo at LOPS. NCEP Reanalysis data provided by the NOAA/OAR/ESRL PSD, Boulder, Colorado, USA, from their Web site (at <https://www.esrl.noaa.gov/psd/>). This study has been conducted using E.U. Copernicus Marine Service Information. More specifically we wish to thank CMEMS for distributing the "Global Ocean Gridded L4 Sea Surface Reprocessed (1993–Ongoing)." Altimeter data were a contribution from the project CNPq 447109/2014-6. NOAA High Resolution SST data provided by the NOAA/OAR/ESRL PSD, Boulder, Colorado, USA (<https://www.esrl.noaa.gov/psd/>). We would like to thank for the distribution of ERAi data the European Centre for Medium-range Weather Forecast (ECMWF) (2011): The ERA-Interim reanalysis data set, Copernicus Climate Change Service (C3S) (accessed on 08/20/2015; available from <https://www.ecmwf.int/en/forecasts/datasets/archive-datasets/reanalysis-datasets/era-interim>). This study was funded by the Fundação de Amparo à Ciência do Estado de São Paulo (FAPESP) under Proc. 2015/26450-8.

### References

- Argo (2018). Argo float data and metadata from Global Data Assembly Centre (Argo GDAC). Retrieved from <https://www.seanoe.org/data/00311/42182/data/60707.tar.gz>. SEANOE, <https://doi.org/10.17882/42182>
- Banzon, V. F., & Reynolds, R. W. (2013). Use of WindSat to extend a microwave-based daily optimum interpolation sea surface temperature time series. *Journal of Climate*, 26(8), 2557–2562. <https://doi.org/10.1175/JCLI-D-12-00628.1>
- CMEMS (2018). SEALEVEL\_GLO\_PHY\_L4\_REP\_OBSERVATIONS\_008\_047. [ftp://my.cmems-du.eu/Core/SEALEVEL\\_GLO\\_PHY\\_L4\\_REP\\_OBSERVATIONS\\_008\\_047/dataset-duacs-rep-global-merged-allsat-phy-l4/E.U.](ftp://my.cmems-du.eu/Core/SEALEVEL_GLO_PHY_L4_REP_OBSERVATIONS_008_047/dataset-duacs-rep-global-merged-allsat-phy-l4/E.U.) Copernicus Marine Service Information
- Davis, X. J., Straneo, F., Kwon, Y. O., Kelly, K. A., & Toole, J. M. (2013). Evolution and formation of North Atlantic Eighteen Degree Water in the Sargasso Sea from moored data. *Deep Sea Research Part II: Topical Studies in Oceanography*.
- de Boyer Montégut, C., Madec, G., Fischer, A. S., Lazar, A., & Iudicone, D. (2004). Mixed layer depth over the global ocean: An examination of profile data and a profile-based climatology. *Journal of Geophysical Research*, 109, C12003. <https://doi.org/10.1029/2004JC002378>
- Dee, D. P., Uppala, S. M., Simmons, A. J., Berrisford, P., Poli, P., Kobayashi, S., et al. (2011). The ERA-Interim reanalysis: Configuration and performance of the data assimilation system. *Quarterly Journal of the Royal Meteorological Society*, 137(656), 553–597.
- Douglass, E. M., Kwon, Y. O., & Jayne, S. R. (2013). A comparison of North Pacific and North Atlantic subtropical mode waters in a climatologically-forced model. *Deep Sea Research Part II: Topical Studies in Oceanography*.
- Ferreira, M. B. (2019). Water temperature, salinity, and other parameters from CTD taken from the research vessel *Cruzeiro do Sul* in the South Atlantic Ocean from 2015-04-01 to 2015-05-08. <http://accession.nodc.noaa.gov/0184862/> NOAA National Centers for Environmental Information. Dataset. (NCEI Accession 0184862).
- Forget, G., Maze, G., Buckley, M., & Marshall, J. (2011). Estimated seasonal cycle of North Atlantic Eighteen Degree Water volume. *Journal of Physical Oceanography*, 41(2), 269–286.
- Gaillard, F., Brion, E., & Charraudeau, R. (2009). ISAS-V5: Description of the Method and User Manual. In *IFREMER Rapport LPO 09-04, Laboratoire de Physique des Océans, UMR 6523 (CNRS-Ifremer-IRD-UBO)*, Plouzane, France pp. 34.
- Garzoli, S. L., & Garraffo, Z. (1989). Transports, frontal motions and eddies at the Brazil-Malvinas Currents Confluence. *Deep Sea Research Part A. Oceanographic Research Papers*, 36(5), 681–703.
- Gordon, A. L. (1981). South Atlantic thermocline ventilation. *Deep Sea Research Part A. Oceanographic Research Papers*, 28(11), 1239–1264.
- Hanawa, K., & Talley, L. D. (2001). Mode Waters. In G. Siedler, J. Church, & J. Gold (Eds.), *Ocean Circulation & Climate* (Vol. 77, pp. 373–386). San Diego, CA: Academic Press.
- Kalnay, E., Kanamitsu, M., Kistler, R., Collins, W., Deaven, D., Gandin, L., et al. (1996). The NCEP/NCAR reanalysis 40-year project. *Bulletin of the American Meteorological Society*, 77(3), 437–471.
- Kelly, K. A., & Dong, S. (2013). The contributions of atmosphere and ocean to North Atlantic Subtropical Mode Water volume anomalies. *Deep Sea Research Part II: Topical Studies in Oceanography*, 91, 111–127.
- Marshall, J., Ferrari, R., Forget, G., Maze, G., Andersson, A., Bates, N., et al. (2009). The CLIMODE field campaign: Observing the cycle of convection and restratification over the Gulf Stream. *Bulletin of the American Meteorological Society*, 90(9), 1337–1350.
- Masuzawa, J. (1969). Subtropical mode water. *Deep Sea Research and Oceanographic Abstracts*, 16(5), 463–468.
- Maze, G., Forget, G., Buckley, M., Marshall, J., & Cerovecki, I. (2009). Using transformation and formation maps to study the role of air-sea heat fluxes in North Atlantic Eighteen Degree Water formation. *Journal of Physical Oceanography*, 39(8), 1818–1835.
- McDougall, T. J., & Barker, P. M. (2011). Getting started with TEOS-10 and the Gibbs Seawater (GSW) oceanographic toolbox. *SCOR/LAPSO WG*, 127, 1–28.
- Provost, C., Escoffier, C., Maamaatuaiahutapu, K., Kartavtseff, A., & Garçon, V. (1999). Subtropical mode waters in the South Atlantic Ocean. *Journal of Geophysical Research*, 104(C9), 21,033–21,049.
- Sato, O. T., & Polito, P. S. (2014). Observation of South Atlantic subtropical mode waters with Argo profiling float data. *Journal of Geophysical Research*, 119, 2860–2881. <https://doi.org/10.1002/2013JC009438>
- Silverthorne, K. E., & Toole, J. M. (2013). Quasi-Lagrangian observations of the upper ocean response to wintertime forcing in the Gulf Stream. *Deep Sea Research Part II: Topical Studies in Oceanography*, 91, 25–34.
- Worthington, L. V. (1972). Negative oceanic heat flux as a cause of water-mass formation. *Journal of Physical Oceanography*, 2(3), 205–211.